Chinese Chemical Letters 35 (2024) 108486

Contents lists available at ScienceDirect

Chinese Chemical Letters

journal homepage: www.elsevier.com/locate/cclet

Parallelogram 3d-4f-5d heterometallic clusters based on trilacunary tungstoantimonates with excellent proton conductivity

Haiying Wang[a], Han Xu[b], Chaolong Chen[c], Yingjie Zhu[a], Yikang Zhang[a], Dongdi Zhang[a,*], Jingyang Niu[a,*]

[a] Henan Key Laboratory of Polyoxometalate Chemistry, College of Chemistry and Molecular Sciences, Henan University, Kaifeng 475004, China
[b] School of Pharmaceutical Science & Yunnan Key Laboratory of Pharmacology for Natural Products, Kunming Medical University, Kunming 650500, China
[c] Collaborative Innovation Center of Chemistry for Energy Materials, State Key Laboratory of Physical Chemistry of Solid Surface and Department of Chemistry, College of Chemistry and Chemical Engineering, Xiamen University, Xiamen 361005, China

ARTICLE INFO

Article history:
Received 20 March 2023
Revised 11 April 2023
Accepted 20 April 2023
Available online 23 April 2023

Keywords:
Polyoxometalate
Parallelogram
Heterometallic
3d-4f-5d cluster
Proton conductivity

ABSTRACT

Two 3d-4f-5d heterometallic cluster-containing polyoxometalates, formulated as $Na_{22}\{(SbW_9O_{33})_4[La_3W_6MO_{18}(H_2O)_8(CH_3COO)_4]_2\}\cdot nH_2O$ (abbreviated as La_6M_2, M = Co/Mn) were synthesized and structurally characterized. Single-crystal X-ray diffraction analyses reveal that the polyanions of La_6Co_2 and La_6Mn_2 consist of the uncommon 3d-4f-5d clusters $\{La_6W_{12}Co_2\}$ and $\{La_6W_{12}Mn_2\}$, which are encapsulated by four trilacunary Keggin tungstoantimonates to form the parallelogram-shaped title compounds. Additionally, the polyanions can be extended into a two-dimensional (2D) frame by the linkage of peripheral Na^+ ions. The inner space of the 2D layer was filled with water molecules and thus an H-bonded network was formed, which is expected to exhibit a fascinating proton conductivity. The study of water-assisted proton conduction demonstrated that La_6Co_2 and La_6Mn_2 were temperature- and humidity-dependent proton conductors, respectively, and the proton conductivities could reach 1.3×10^{-2} and 2.3×10^{-2} S/cm at 65 °C and 90% RH conditions.

© 2024 Published by Elsevier B.V. on behalf of Chinese Chemical Society and Institute of Materia Medica, Chinese Academy of Medical Sciences.

Polyoxometalates (POMs) are a class of anion metal oxygen clusters composed of early transition-metal, and have brought remarkable advances in catalysis, magnetism, biomedicine, materials science, and nanotechnology [1–12]. Generally, saturated POM clusters can be transformed into lacunary building blocks by removal of one or more $\{XO_6\}$ octahedra under given conditions. The terminal oxygen at the lacunary site has strong nucleophilic nature because of its improved charge density. Therefore, lacunary POM derivatives are ideal candidates to coordinate with electrophilic transition (3d) or rare-earth (4f) metals [13]. However, their utilization is still limited isometallic cluster-incorporation POM derivatives, such as the representative high-nuclear 3d or 4f cluster-incorporation species $\{Mn_{40}P_{32}W_{224}\}$ [14], $\{Fe_{28}P_8W_{48}\}$ [15], $\{Co_{16}(PW_9)_4\}$ [16], $\{Ni_{25}(SiW_9)_6\}$, [17] $\{Cu_{20}(P_8W_{48})\}$ [18], $\{Ce_{20}Ge_{10}W_{100}\}$ [19] and $\{Ln_{27}Ge_{10}W_{106}\}$ (Ln: La, Ce) [20].

The 3d-4f or 4d-4f heterometallic aggregates occupy a special place among POM-based molecular materials not only because of their inherent contributions of electrons, but also owing to the increasing exchange phenomenon between the 3d/4d and 4f centers [21–26]. Notably, most heterometallic aggregates-containing POM complexes (HMPOMs), especially for discrete molecular clusters, were restricted to binary mixed systems. From the viewpoint of POM structure, although dimeric or trimeric HMPOMs have been widely communicated, there are only four tetrameric HMPOMs (Fig. S1 in Supporting information) [27–30]. To our knowledge, no examples of POM-based trinary heterometallic aggregates have been reported so far. Therefore, it is a challenge to explore suitable synthetic conditions to incorporate 3d-4f-5d or 4d-4f-5d heterometallic aggregates into POM ligands.

The Lewis basicity of oxygen atom can form cation-cationic interactions with Lewis acidity of 3d or 4f centers, and thus act as hydrogen bond receptors to result in the excellent proton conductivity [31]. As a continuous interest in 3d-4f-POM systems [23,24,29], we herein present the synthesis and characterization of two unprecedented 3d-4f-5d HMPOMs $Na_{22}[(SbW_9O_{33})_4\{La_3W_6MO_{18}(H_2O)_8(CH_3COO)_4\}_2]\cdot nH_2O$(abbreviated as La_6Co_2, $n = 60$; La_6Mn_2, $n = 75$), which have remarkable features: (1) Comprise a distinct 3d-4f-5d aggregate $\{La_6W_{12}M_2\}$ (M = Co/Mn), showing a structure novel for the polyanion chemistry of heterometallic clusters; (2) Display an unusual parallelogram tetrameric structure with dimension of *ca.* $2.3 \times 1.8 \times 2.6$

* Corresponding authors.
E-mail addresses: ddzhang@henu.edu.cn (D. Zhang), jyniu@henu.edu.cn (J. Niu).

https://doi.org/10.1016/j.cclet.2023.108486
1001-8417/© 2024 Published by Elsevier B.V. on behalf of Chinese Chemical Society and Institute of Materia Medica, Chinese Academy of Medical Sciences.

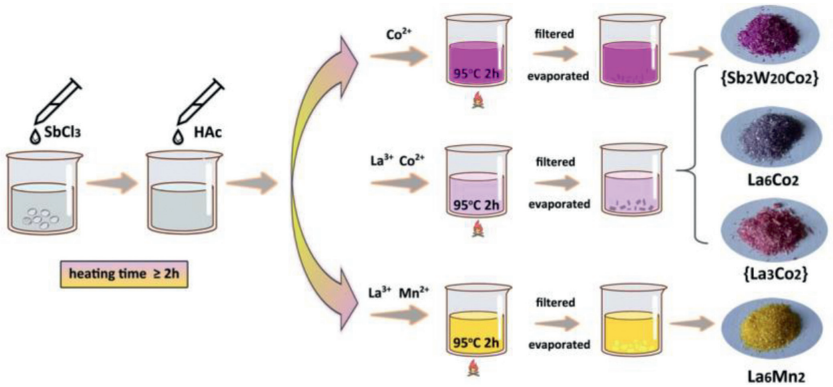

Scheme 1. The synthetic route of La_6M_2, highlighting the different processes of La_6Co_2, $\{Sb_2W_{20}Co_2\}$ and $\{La_3Co_2\}$.

nm^3 (Fig. S3 in Supporting information); (3) Represent the first Mn-4f heterometallic cluster in tungstoantimonate chemistry (Fig. S2 and Table S1 in Supporting information) [29,30,32–37]; (4) Show excellent proton conductivity at 65 °C and 90% RH.

Trilacunary tungstoantimonate ($[SbW_9O_{33}]^{9-}$) was chosen as the POM building block because it offers a well-known affinity towards 3d or 4f electrophiles. More importantly, the presence of lone-pair electrons can prevent the formation of a fully closed saturated structure, which is in favor of forming high polymeric compounds [38]. As shown in Scheme 1, La_6Co_2 and La_6Mn_2 were synthesized by the subsequent addition of $LaCl_3{\cdot}7H_2O$ and $CoCl_2{\cdot}6H_2O$ or $MnCl_2{\cdot}4H_2O$ into the *in-situ* formed $[SbW_9O_{33}]^{9-}$ solution. Notably, the same reaction leads to the formation of complex $\{Sb_2W_{20}Co_2\}$ (Scheme 1 and Fig. S4 in Supporting information) without addition of La^{3+} [39]. Furthermore, a small amount of $\{La_3Co_2\}$ (Scheme 1 and Fig. S4) [30] and $\{Sb_2W_{20}Co_2\}$ [39] can be also isolated after the crystallization of La_6Co_2. We also found that the more La^{3+} is added, the less $\{La_3Co_2\}$ is formed. Luckily, the three compounds can be easily distinguished by their different colors (Scheme 1 and Fig. S4). However, La_6Mn_2 is exclusively formed in the La/Mn system, indicating that the metal ion may play an essential role in regulating composition of the structure, which in turn guides the formation of HMPOMs. To some extent, the successful synthesis of La_6Co_2 and La_6Mn_2 may "open" a synthetic route to a new class of heterometallic clusters, giving access to novel building blocks that can be universally used to assemble clusters with a remarkable range of structures and properties.

Single-crystal structural analyses reveal that the polyanions of La_6Co_2 and La_6Mn_2 are isostructural and crystallize in the same monoclinic space group *C2/c* (Table S2 in Supporting information). Therefore, only the structure of the polyanion of La_6Mn_2 is described in detail. As shown in Fig. 1, this cluster can be viewed as a tetrameric Keggin polyoxotungstate, in which a huge 3d-4f-5d heterometallic cluster $\{[La_3W_6MnO_{18}(H_2O)_8(CH_3COO)_4]_2\}$ ($\{La_6W_{12}Mn_2\}$, Fig. 1c) are wrapped by four inorganic ligands (two $\{\beta$-B-$SbW_9O_{33}\}$ (Fig. 1a) and two $\{\alpha$-A-$SbW_9O_{33}\}$ (Fig. 1b)). The four Keggin fragments are linked to each other in a parallelogram-like manner (Fig. 1d and Fig. S3), in which the two identical fragments are located at the opposite vertex position. Each $\{\beta$-B-$SbW_9O_{33}\}$ fragment is linked to $\{La_6W_{12}Mn_2\}$ core by four W-O-W bridges and two Mn-O-W bridges, while two additional La-O-W bridges are required between $\{\alpha$-A-$SbW_9O_{33}\}$ cluster and $\{La_6W_{12}Mn_2\}$ core (Figs. S5 and S6 in Supporting information). The $\{La_6W_{12}Mn_2\}$ core contains two MnO_6 octahedra (Fig. 1e), two $\{W_6O_{28}\}$ clusters (Fig. 1f) and two $\{La_3O_{24}\}$ species (Fig. 1g), resulting the first observation of 3d-4f-5d heterometallic cluster in POM chemistry. All the W and Mn atoms have octahedral coordination of oxygen atoms, while the La atoms exhibit three different coordination geometries, nine-coordination tricapped trigonal prism (Fig. S7a in Supporting information), ten-coordination double-capped tetragonal antiprism (Fig. S7b in Supporting information), and nine-coordination single-capped tetragonal antiprism (Fig. S7c in Supporting information), respectively. Notably, La_6Mn_2 represents the first example of Mn-4f mixed-cluster in tungstoantimonate chemistry.

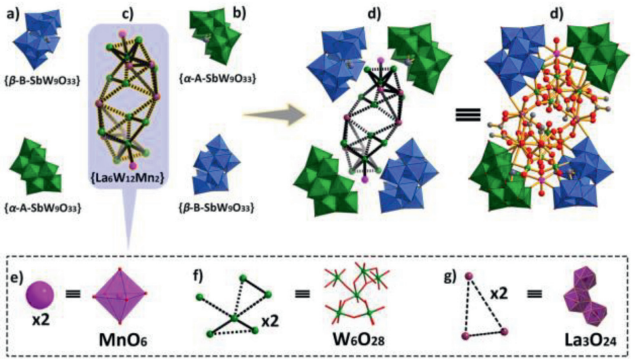

Fig. 1. The structure of (a) $\{\beta$-B-$SbW_9O_{33}\}$, (b) $\{\alpha$-A-$SbW_9O_{33}\}$, (c) $\{La_6W_{12}Mn_2\}$, polyanion in (d) La_6Mn_2, (e) $\{MnO_6\}$, (f) $\{W_6O_{28}\}$ and (g) $\{La_3O_{24}\}$. Code: $\{WO_6\}$, blue/green octahedra; C, gray spheres; O, red spheres; Sb, gray-purple spheres; W, green spheres; Mn, rosy spheres; La, violet spheres.

The structure of the polyanion of La_6Mn_2 can be also described as comprising two dimeric half-units $[(SbW_9O_{33})_2\{La_3W_6MnO_{21}(H_2O)_8(CH_3COO)_4\}]^{17-}$ (Fig. S5), in which two trilacunary tungstoantimonate fragments are supported on the unprecedented heterometallic complex $[La_3W_6MnO_{21}(H_2O)_8(CH_3COO)_4]^{+}$ through one corner-shared $\{MnO_6\}$ octahedra, four W-O-W bridges and two La-O-W bridges. Two half-units are fused together *via* two La centers, and the apparent 180° rotation of the half-unit leads to a staggered tetragon.

Bond valence sum (BVS) calculations (Table S3 in Supporting information) [40] indicate that the Sb, W, La, Co and Mn atoms in compound La_6Co_2 and La_6Mn_2 are all in the +3, +6, +3, +2 and +2 oxidation state, respectively. Furthermore, the BVS calculations for all oxygen atoms in La_6Co_2 and La_6Mn_2 enable us to identify the presence of the eight terminal aqua ligands with values of 0.28–0.38. The resulting $[(SbW_9O_{33})_4\{La_3W_6MO_{18}(H_2O)_8(CH_3COO)_4\}_2]^{22-}$ (M = Co/Mn) polyanions are perfectly charge-balanced with 22 sodium cations, in agreement with the results of elemental analysis.

In La_6M_2, polyanions can be extended into a 2D metal framework if the peripheral Na^+ ions are regarded as linkers (Fig. S9 in Supporting information). In addition, there are a large number of crystal water molecules in and between the 2D planes

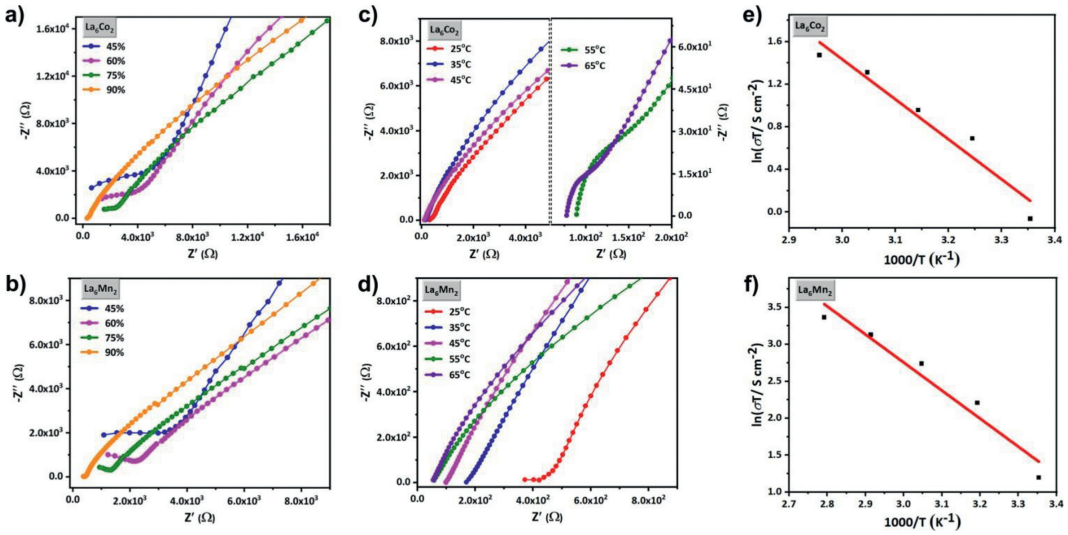

Fig. 2. (a, b) Impedance spectra of La_6M_2 at 25 °C with 45%–90% RHs. (c, d) Impedance spectra at 90% RH with 25–65 °C. (e, f) Arrhenius plots of proton conductivity for La_6M_2 under 90% RH.

(Fig. S10 in Supporting information). Therefore, a hydrogen-bonded network would be formed by abundant water molecules, countercations and polyanions, used for proton transmission. Simultaneously, the unique "pseudoliquid pase" behavior of POMs [41] was also its unique advantage as a proton conductive material. Herein, the proton conductivity of La_6M_2 was investigated by AC impedance measurement using compacted pellets of the crystalline powder samples at relative humidity (RH) and temperature in a range of 45%–90% and 25–65 °C, respectively. Figs. 2a and b show the real (Z') and imaginary ($-Z''$) spectra of La_6M_2 in the RH range of 45%–90% at 25 °C. Proton conductivity (σ) of La_6Co_2 increased from 2.3×10^{-4} S/cm to 3.2×10^{-3} S/cm when RH was increased from 45% to 90%. Under the same conditions, σ of La_6Mn_2 was increased from 3.8×10^{-4} S/cm to 2.6×10^{-3} S/cm, which was in the same order of magnitude as that of La_6Co_2. Similar conductivity was to be expected due to isomorphous crystals and similar void ratio of La_6Co_2 (28.1%) and La_6Mn_2 (27.8%). The water vapor adsorption tests of La_6M_2 showed positive interrelationships between water adsorption and RH (Fig. S11 in Supporting information). At 298 K and $P/P_0 = 0.90$, the water vapor adsorption capacity of La_6M_2 reached 74 cm^3/g and 83 cm^3/g, respectively. When maximum adsorption capacity was reached, proton conductivity also reached the maximum value, indicating that there was positive interrelationship between water adsorption and proton conduction. Furthermore, as shown in Figs. S12 and S13 (Supporting information), PXRD peaks of as-synthesized compound before and after proton conductivity measurement were basically in agreement with the corresponding simulated peaks, indicating that the structure of La_6M_2 remained intact during the measurement.

Temperature-dependent conductivity measurements were carried out in temperatures ranging from 25 °C to 65 °C under 90% RH. Upon rising temperature to 65 °C, conductivity increased to 1.3×10^{-2} and 2.3×10^{-2} S/cm for La_6Co_2 and La_6Mn_2, respectively (Figs. 2c and d). The elevated conductivities were attributed to the acceleration of water molecular motion at high temperatures [42]. Notably, at 65 °C and 90% RH, the conductivities of La_6M_2 show excellent conductivity among reported POM conductive materials [43,44]. According to the Arrhenius equation ($\sigma T = \sigma_0 \exp(-E_a/k_b T)$), activation energy ($E_a$) at 90% RH for La_6Co_2 and La_6Mn_2 were calculated to be 0.324 eV and 0.327 eV (<0.4 eV) (Figs. 2e and f), respectively, suggesting that conduction proceeds were mainly dominated by Grotthuss mechanism [45,46], and protons were hopping along conductivity pathway.

In summary, we report the construction of two unprecedented HMPOMs, in which four trilacunary tungstoantimonate building units are efficiently linked by the rare hybrid 3d-4f-5d cluster $\{La_6W_{12}M_2\}$ (M = Co/Mn) to form a parallelogram tetrameric architecture. In our case, polyanion La_6Mn_2 represents the first heterometallic 3d-4f cluster in tungstoantimonate chemistry. More importantly, the new compounds are of interest in their excellent proton conductivity due to their 2D layer filled with water molecules, which is favorable to form an H-bonded network. The fact that 3d, 4f and 5d metals can be simultaneously incorporated into the lacunary POM structure extends the work to the systematic study of other 4f or 5f ions into this multicomponent system in order to achieve a better understanding of the interaction between lacuanry POM clusters and 3d/4f/5f centers.

Declaration of competing interest

The authors declare that they have no known competing financial interests or personal relationships that could have appeared to influence the work reported in this paper.

Acknowledgments

This work was supported by the National Natural Science Foundation of China (No. 22071045), the Excellent Youth Science Fund Project of Henan Province (No. 202300410042), the Natural Science Foundation of Henan Province (No. 232300420372), Henan University, and the State Key Laboratory of Physical Chemistry of the Solid Surface of Xiamen University.

Supplementary materials

Supplementary material associated with this article can be found, in the online version, at doi:10.1016/j.cclet.2023.108486.

References

[1] M.T. Pope, A. Müller, Angew. Chem. Int. Ed. 30 (1991) 34–48.
[2] H.N. Miras, J. Yan, D.L. Long, L. Cronin, Chem. Soc. Rev. 41 (2012) 7403–7430.
[3] M. Lu, M. Zhang, J. Liu, et al., J. Am. Chem. Soc. 144 (2022) 1861–1871.
[4] L. Qin, R. Wang, X. Xin, et al., Appl. Catal. B: Environ. 312 (2022) 121386.
[5] J. Li, D. Zhang, Y. Chi, C. Hu, Polyoxometalates 1 (2022) 9140012.
[6] Y. Wang, Y. Lu, W. Zhang, et al., Polyoxometalates 1 (2022) 9140005.
[7] L. Qin, C. Zhao, L.Y. Yao, et al., CCS Chem. 4 (2022) 259–271.
[8] Z. Wang, X. Xin, M. Zhang, et al., Sci. China Chem. 65 (2022) 1515–1525.

[9] L. Qiao, M. Song, A. Geng, S. Yao, Chin. Chem. Lett. 30 (2019) 1273–1276.
[10] Z.M. Zhang, X. Duan, S. Yao, et al., Chem. Sci. 7 (2016) 4220–4229.
[11] L. Yang, Z. Zhang, C. Zhang, et al., Inorg. Chem. Front. 9 (2022) 4824–4833.
[12] D. Cheng, Z. Gao, W. Wang, et al., Polyoxometalates 2 (2023) 9140019.
[13] L.L. Li, H.Y. Han, Y.H. Wang, et al., Dalton Trans. 44 (2015) 11429–11436.
[14] X. Fang, P. Kögerler, Y. Furukawa, M. Speldrich, M. Luban, Angew. Chem. Int. Ed. 123 (2011) 5318–5322.
[15] B. Godin, Y.G. Chen, J. Vaissermann, et al., Angew. Chem. Int. Ed. 117 (2005) 3132–3135.
[16] M. Ibrahim, Y. Lan, B.S. Bassil, et al., Angew. Chem. Int. Ed. 123 (2011) 4805–4808.
[17] X.B. Han, Y.G. Li, Z.M. Zhang, et al., J. Am. Chem. Soc. 137 (2015) 5486–5493.
[18] S.S. Mal, U. Kortz, Angew. Chem. Int. Ed. 44 (2005) 3777–3780.
[19] B.S. Bassil, M.H. Dickman, I. Römer, B. von der Kammer, U. Kortz, Angew. Chem. Int. Ed. 46 (2007) 6192–6195.
[20] Z. Li, X.X. Li, T. Yang, Z.W. Cai, S.T. Zheng, Angew. Chem. Int. Ed. 56 (2017) 2664–2669.
[21] M. Ibrahim, V. Mereacre, N. Leblanc, et al., Angew. Chem. Int. Ed. 54 (2015) 15574–15578.
[22] M. Ibrahim, Y. Peng, E. Moreno-Pineda, et al., Small Struct. 2 (2021) 2100052.
[23] S.R. Li, H.Y. Wang, H.F. Su, et al., Small Methods 5 (2021) 2000777.
[24] S. Li, Z. Weng, L. Jiang, et al., Chin. Chem. Lett. 34 (2023) 107251.
[25] Y.N. Gu, Y. Chen, Y.L. Wu, S.T. Zheng, X.X. Li, Inorg. Chem. 57 (2018) 2472–2479.
[26] S.R. Li, W.D. Liu, L.S. Long, L.S. Zheng, X.J. Kong, Polyoxometalates 2 (2023) 9140022.
[27] G. Xue, B. Liu, H. Hu, et al., J. Mol. Struct. 690 (2004) 95–103.
[28] A.H. Ismail, B.S. Bassil, G.H. Yassin, B. Keita, U. Kortz, Chem. Eur. J. 18 (2012) 6163–6166.
[29] J. Cai, X.Y. Zheng, J. Xie, et al., Inorg. Chem. 56 (2017) 8439–8445.
[30] B. Artetxe, S. Reinoso, L. San Felices, et al., Chem. Eur. J. 22 (2016) 4616–4625.
[31] D. Gui, W. Duan, J. Shu, et al., CCS Chem. 1 (2019) 197–206.
[32] J.W. Zhao, J. Cao, Y.Z. Li, J. Zhang, L.J. Chen, Cryst. Growth Des. 14 (2014) 6217–6229.
[33] S. Yao, J.H. Yan, H. Duan, et al., RSC Adv. 5 (2015) 76206–76210.
[34] L. Chen, J. Cao, X. Li, et al., CrystEngComm 17 (2015) 5002–5013.
[35] E. Tanuhadi, E. Al-Sayed, G. Novitchi, et al., Inorg. Chem. 59 (2020) 8461–8467.
[36] J. Cai, R. Ye, X. Liu, L. Guo, X. Qiao, Dalton Trans. 49 (2020) 16954–16961.
[37] B. Zeng, Y. Zhang, Y. Chen, et al., Inorg. Chem. 60 (2021) 2663–2671.
[38] E. Tanuhadi, N.I. Gumerova, A. Prado-Roller, A. Mautner, A. Rompel, Inorg. Chem. 60 (2021) 8917–8923.
[39] M. Bösing, I. Loose, H. Pohlmann, B. Krebs, Chem. Eur. J. 3 (1997) 1232–1237.
[40] I.D. Brown, D. Altermatt, Acta Crystallogr. B 41 (1985) 244–247.
[41] S.S. Wang, G.Y. Yang, Chem. Rev. 115 (2015) 4893–4962.
[42] W. Ma, B. Hu, K. Jing, et al., Dalton Trans. 49 (2020) 3849–3855.
[43] N. Ogiwara, T. Iwano, T. Ito, S. Uchida, Coord. Chem. Rev. 462 (2022) 214524.
[44] M. Zhu, T. Iwano, M. Tan, et al., Angew. Chem. Int. Ed. 61 (2022) e202200666.
[45] K.D. Kreuer, A. Rabenau, W. Weppner, Angew. Chem. Int. Ed. 94 (2006) 224–225.
[46] D.W. Lim, H. Kitagawa, Chem. Rev. 120 (2020) 8416–8467.